

Published in final edited form as:

*Laryngoscope*. 2011 August ; 121(8): 1687–1701. doi:10.1002/lary.21856.

## Immunohistochemical characterization of human olfactory tissue

Eric H. Holbrook, M.D.<sup>1</sup>, Enming Wu, B.S.<sup>2</sup>, William T. Curry, M.D.<sup>3</sup>, Derrick T. Lin, M.D.<sup>1</sup>, and James E. Schwob, M.D., Ph.D.<sup>2</sup>

<sup>1</sup>Department of Otolaryngology, Harvard Medical School, Massachusetts Eye and Ear Infirmary, Boston, Massachusetts

<sup>2</sup>Department of Anatomy and Cellular Biology, Tufts University School of Medicine, Boston, Massachusetts

<sup>3</sup>Department of Surgery (Neurosurgery), Harvard Medical School, Massachusetts General Hospital, Boston, Massachusetts

### Abstract

**Objectives/Hypothesis**—The pathophysiology underlying human olfactory disorders is poorly understood because biopsying the olfactory epithelium (OE) can be unrepresentative and extensive immunohistochemical analysis is lacking. Autopsy tissue enriches our grasp of normal and abnormal olfactory immunohistology and guides the sampling of the OE by biopsy. Furthermore, a comparison of the molecular phenotype of olfactory epithelial cells between rodents and humans will improve our ability to correlate human histopathology with olfactory dysfunction.

**Study Design**—An immunohistochemical analysis of human olfactory tissue using a comprehensive battery of proven antibodies.

**Methods**—Human olfactory mucosa obtained from 21 autopsy specimens was analyzed with immunohistochemistry. The position and extent of olfactory mucosa was assayed by staining whole mounts with neuronal markers. Sections of the OE were analyzed with an extensive group of antibodies directed against cytoskeletal proteins and transcription factors, as were surgical specimens from an esthesioneuroblastoma.

**Results**—Neuron-rich epithelium is always found inferior to the cribriform plate, even at advanced age, despite the interruptions in the neuroepithelial sheet caused by patchy respiratory metaplasia. The pattern of immunostaining with our antibody panel identifies two distinct types of basal cell progenitors in human OE similar to rodents. The panel also clarifies the complex composition of the esthesioneuroblastoma.

**Conclusion**—The extent of human olfactory mucosa at autopsy can easily be delineated as a function of age and neurological disease. The similarities in human vs. rodent OE will enable us to translate knowledge from experimental animals to humans and will extend our understanding of human olfactory pathophysiology.

### Keywords

esthesioneuroblastoma; cytoskeletal proteins; cell division; transcription factors; autopsy

---

Corresponding Author: Eric H. Holbrook, M.D., 243 Charles Street, Boston, MA, 02114, Ph. 617-573-3209, Fax 617-573-3914, eric\_holbrook@mei.harvard.edu.

Financial Disclosure: None of the authors have any financial interest in companies or other entities that may have an interest in this work. There are no conflicts of interest to disclose for any of the authors.

## Introduction

Our understanding of the basic principles of olfactory physiology has grown tremendously over the years. With recent molecular advances and new lineage tracing technologies, we can begin to understand the complex interactions among the various cell types of the olfactory epithelium (OE) and identify signals that regulate cell fate. Olfactory epithelial neurogenesis appears to be a tightly regulated process that is necessary for maintaining olfactory function in a tissue vulnerable to environmental insults throughout life. But even with the successes of recent years, we have very little understanding as to the pathophysiology of the most common forms of olfactory sensory loss in humans.

A large part of our ignorance stems from the paucity of sufficient anatomical and pathological analyses of biopsy and autopsy material. Given the observed patchy replacement of olfactory mucosa, the severity of which may be related to age<sup>1-3</sup>, the limited size of material typically obtained at biopsy, and difficulty in obtaining the biopsies without distortion of the sample, it should be no surprise that the yield of interpretable olfactory tissue in previous studies has been low<sup>4</sup>. It also raises a concern that the conclusions relating biopsy findings to clinical olfactory function may be invalidated by sampling error. Better assessment of the olfactory organ as a whole is needed to correlate dysfunction with histology<sup>5</sup>, accurately, which is admittedly difficult to achieve in living subjects. However, a better characterization of the area within the nasal cavity that contains the most representative population of olfactory neurons (ONs) would increase our ability to capture true olfactory mucosa more consistently. In addition, a broader analysis of the biopsied OE beyond a simple evaluation as to the presence or absence of neurons is critical given the dynamic nature of this neuroepithelium. Antibodies to cell signaling proteins and transcription factors already known to regulate various aspects of development, neurogenesis and epithelial reconstruction in the OE of rodents may also be useful in providing valuable clues as to the pathophysiology underlying olfactory disorders and possibly olfactory tumorigenesis.

Accordingly, we performed immunohistochemistry on whole mounts (WM) of mucosa obtained from human nasal autopsy tissue and here describe areas consistently rich in ONs. We then used an extensive battery of antibodies for immunohistochemical analysis of OE sections obtained from autopsy material and describe the detailed pattern of staining. Our results suggest that the staining properties in human OE are remarkably similar to those described in rodents. We further show that these antibodies can also provide novel insights into the composition of esthesioneuroblastoma and suggest further avenues for exploring the cellular origin of the tissue.

## Methods

This study was approved by the Institutional Review Board (IRB) of Massachusetts Eye and Ear Infirmary and Tufts University School of Medicine. The protocol was considered exempt from requiring informed consent.

### Autopsy specimens

Whole block autopsy specimens of human olfactory tissue were obtained through the National Disease Research Interchange (NDRI, Philadelphia, PA) using a protocol to harvest a block of tissue from the nasal cavity that extends from the frontal sinus anteriorly, to the sphenoid sinus posteriorly, and from the cribriform plate (including the olfactory bulbs), to the nasal floor. The lateral extent included the medial wall of the maxillary sinuses. Specimens were immediately placed in 10% formalin at the procurement center, sent to NDRI for testing and packaging, and arrived at our lab within 14–21 days. Twenty-one

specimens (8 females) were obtained with an age range of 49–96 years (mean = 77). Subjects with a history of nasal/sinus surgery, anterior skull base surgery or malignancy, radiation to the nose/sinuses, or history of nasal cocaine abuse were excluded. Smoking history was not chosen as an exclusion criterion in order to ensure adequate numbers of specimens. Autopsies and tissue harvesting were all performed with a postmortem interval of 24 hours or less. Brief medical histories and cause of death were provided with each specimen.

The specimens were dissected upon arrival to our lab. The lateral walls of the nasal cavity including the turbinates were carefully separated from the septum by making sharp cuts from the sphenoid ostium along the skull base and cribriform plate on each side of the septum to the frontal sinus ostium. Inferior cuts were made from the sphenoid sinus ostium to the choana and from the frontal sinus floor and root of the nasal bones to the superior nasal cavity. Pictures were then taken of both sides of the septum and lateral nasal walls using a handheld digital camera (Sony Cybershot F717, Japan) using macro settings. Rectangular portions of mucosa (approximately 30 mm × 15 mm) positioned below the cribriform plate and extending posteriorly to the face of the sphenoid were carefully stripped from the underlying bone and cartilage of the septum and bone of the lateral walls/turbinates on each side and were used for WM immunohistochemical staining. A smaller, vertically-oriented rectangular piece of mucosa was excised from each of the larger specimens from the superior extent of the sample below the middle of the cribriform plate (Fig. 1A). A vertically oriented excision was designed to incorporate the respiratory/olfactory epithelial junction. The smaller samples were processed for cryosectioning and immunohistochemistry. A 1.5 × 1.5 mm square of tissue was then removed from the anterior-inferior corner of the larger mucosa specimen for orientation purposes. Photographs of the harvested tissue block were repeated to document the extent of the mucosal excision permitting later assessment of regional staining patterns of olfactory epithelium by comparison with the nasal anatomy as a whole.

### **Esthesioneuroblastoma specimen**

A 3 × 3 cm portion of biopsy-verified esthesioneuroblastoma tissue was obtained from a 44 year-old female at the time of a craniofacial resection of the tumor. The surgery was performed prior to radiation or chemotherapy. The final diagnosis was esthesioneuroblastoma, Hyams grade II. The specimen was quickly rinsed in normal saline and transferred to sterile DMEM culture medium with Hepes Buffer (Gibco/Invitrogen, Carlsbad, CA) and brought to the lab for further processing. A portion of the specimen was removed and placed in 4% fresh paraformaldehyde fix for 6 days at 4°C and then placed in phosphate buffered saline (PBS) to be processed for cryosectioning.

### **Cryosectioning**

Both the mucosal and tumor specimens were cryoprotected in 30% sucrose in PBS overnight and snap frozen with liquid nitrogen in OCT compound (Miles Inc., Elkhart, IN). The small mucosal specimens were carefully oriented for coronal sectioning of the epithelium, frozen, and then cut at 12 μm thickness using a cryostat (Leica CM3050S, Bannockburn, IL). The tumor specimens were cut at 8 μm thickness. Sections from both tissues were collected on Plus slides (Fisher Scientific, Pittsburg, PA) and stored at –20°C for future use.

### **Immunohistochemistry**

In general, the steps for immunohistochemistry of the WM and sections were similar in terms of sequence (with a few exceptions which are specified), but longer incubation times for the WM tissue were required to allow for better tissue penetration. Frozen sections were rinsed in PBS for 5 minutes to remove the OCT. Hydrogen peroxide was used at 0.1% for 10

minutes to quench inherent peroxidase activity. Sections were puddled with 0.01 M citric acid buffer (pH 6.0), and placed in a commercial food steamer containing water in its reservoir heated to 90°C for 10 minutes. Sections were then rinsed in PBS and then incubated in a blocking solution (10% donkey serum + 5% nonfat dry milk + 4% BSA + 0.1% Triton X-100) for ten minutes. Incubation with primary antibodies (Table I) occurred overnight at 4°C. Bound primary antibodies were visualized either by incubation with the corresponding biotinylated secondary antibody (Jackson ImmunoResearch Laboratories, Inc., West Grove, PA) followed by avidin-bHRP conjugate (Elite ABC Kit; Vector Laboratory, Burlingame, CA) and then 3,3'-diamino-benzidine (DAB) as a chromagen or with one of several fluorescently conjugated secondary antibodies (Invitrogen, Carlsbad, CA) for purposes of co-localization by double labeling. Tyramide signal amplification was utilized to enhance Mash1 and Notch1 fluorescent signals according to kit instructions (PerkinElmer, Waltham, MA). Fluorescent sections were additionally stained for nuclei using DAPI or Hoechst staining. Some sections stained with DAB were counterstained with hematoxylin.

WMs were incubated in 3% hydrogen peroxide for one hour and then dehydrated and re-hydrated through sequential dilutions of ethanol for 20 minutes each prior to staining. They were then submerged in blocking solution overnight and the solution was then switched to a primary antibody solution consisting of the block solution containing PGP9.5 (1:7,000) and 0.01% sodium azide (to prevent bacterial overgrowth) for 5–6 days at 4° C. Detection of the antibody staining using DAB was as described above for tissue sections. WMs were flattened on poly-L-lysine coated slides after incubation in a 10% glycerine/PBS solution for 2 days and dehydrated to xylene prior to coverslipping.

## Photography

Sections and low power magnified views of the whole mount were imaged with a Spot RT color digital camera (Spot, Sterling Heights, MI) attached to a Nikon 800 E microscope (Nikon Instruments Inc., Melville, NY). Image preparation, assembly, and analysis were performed in Adobe Photoshop CS2 and CS3 (Adobe Systems Incorporated, San Jose, CA). In all cases, only balance, contrast, brightness, and evenness of illumination were altered. Cartoon images of the WM staining used in Figure 1A were obtained from a mosaic of low power photographs reconstructed with IPLab imaging software (BioVision Technologies, Exton, PA).

## Results

### Immunohistochemical analysis of mucosal whole mounts

A more comprehensive understanding of the stem and progenitor cells of the human olfactory epithelium required a global examination of the position and extent of the olfactory mucosa in autopsy specimens, which is poorly understood at best. To that end, WM specimens of mucosa were detached from the septum and lateral wall of the nasal cavity and were stained with an antibody directed against protein gene product 9.5 (PGP9.5), which is commonly used as a neuron- or paraneuron-specific marker. As a consequence, the pattern and extent of olfactory epithelium can be directly mapped onto the walls of the nasal cavity. Prior to staining, a thin rectangular portion was removed from the middle of the WM specimen for crysectioning and immunohistochemistry. As reported previously<sup>1</sup>, the human olfactory mucosa was generally located in the upper nasal cavity below the cribriform plate (Fig. 1A). In our mostly elderly adult specimens (> 65 years), regions rich in olfactory neurons often extended back to the face of the sphenoid sinus with an overall length sometimes approaching 2 cm and vertical dimensions greater than 1 cm. Areas that lacked PGP9.5(+) cells were interspersed and interrupted the continuity of the neuron-containing

olfactory mucosa especially near the borders of the olfactory region (Fig. 1A and inset) as has been previously reported<sup>1</sup>. These aneuronal lacunae were variable in size and extent but were usually roughly circular. Small discontinuities in the sheet of PGP-stained cells were also observed, which likely correspond to ducts of Bowman's glands and/or "olfactory pits" based on our comparisons with histological sections harvested from the tissue; these, too, have been described previously<sup>6</sup>.

Whereas PGP9.5 staining of the whole mount tissue delimits the neuroepithelium and its dense population of neurons, closer inspection of the epithelium surrounding this area reveals sporadic and isolated PGP9.5-stained cells that do not look like neurons. These PGP9.5(+) non-neuronal cells co-label with a marker for respiratory epithelium (see Fig. 2E,F,G) and do not express other neuronal markers at a detectable level. Nonetheless, olfactory mucosa can be identified in the WMs with confidence using PGP9.5 staining by taking into account the density of stained cells and whether their shape is characteristic of olfactory neurons. In large part, the correlation of WM appearance and a detailed comparison of PGP staining in cryosections with that of other highly specific olfactory neuronal markers, including neuron specific tubulin (Tuj-1), olfactory marker protein (OMP) and the neural cell adhesion molecule (NCAM), guides the observer in defining neuron-containing from aneuronal epithelium.

By labeling sections with markers for both mature and immature neurons, we can attempt to assess the overall regenerative state of the epithelium. In the case of a stained WM harvested from a 75 year-old male with Alzheimer's Disease, immunohistochemical analysis of sections obtained from a strip of mucosa within the olfactory region demonstrates a rich population of PGP9.5(+) olfactory neurons but very few mature, OMP(+) cells (Fig 1B). In contrast, other specimens are characterized by a more normal appearing epithelium that encompasses a large number of OMP(+) neurons (see Figs. 4D, E, F). In general, the appearance within each specimen will include areas where the epithelium is dominated by immature neurons, intercalated patches of aneuronal epithelium, and areas of more "normal" appearing epithelium with abundant mature neurons, but the relative preponderance of one type varied between specimens.

### **Immunohistochemical classification of cell types within the human olfactory mucosa**

A comprehensive understanding of the status of the olfactory mucosa in health and disease requires an analysis of all of the constituent cell types. To that end, and based on studies of the olfactory and respiratory mucosa in rodents, a cohort of antibodies was chosen that can be used either simply or in combination to mark each of the cell types of the epithelium. The cell type specific markers include transcription factors, cytoskeleton proteins, and cell-surface glycoproteins, some of which have been used in the past<sup>5,7,8</sup>. A number of published studies have used one or several reagents to characterize the cellular composition and the condition of the human OE. Surprisingly, several of the reagents seemingly produce staining patterns that are interpreted as different from what we and others have described in the rodent OE. Accordingly, we have examined, or re-examined quite closely, the question of which cell types are stained with which antibodies and used multiple reagents to determine the molecular signature of the several cell types. In contrast to some reports from other laboratories, we show here that, in general, the immunohistochemical staining patterns with the marker antibodies were highly similar to those found in rodent tissue. Each of the staining properties of each of the various cell types is described in turn.

**Sustentacular cells and Bowman's glands and ducts**—These cell types are closely related and seemingly generated, at least in part, from a common progenitor cell during recovery after epithelial injury<sup>9,10</sup>. Staining for the anti-neurogenic basic helix-loop-helix

transcription factor Hes1 labels nuclei of the supporting cells at the apical layer of the epithelium as in rats and mice (Fig. 2A). By comparison, antibodies against the transcription factor Sox9 labeled nuclei of Bowman's duct and gland cells exclusively (Fig. 2B), again as exactly seen in rodents. We were surprised to find that even under the suboptimal conditions expected of autopsy material, immunohistochemical labeling of these and other transcription factors was strong.

Staining of the epithelium with keratin 18 (K18) antibodies labeled all three cell types: supporting cells and Bowman's duct and gland cells (Fig. 2C). In addition to K18, labeling with an antibody against the cell adhesion protein E-cadherin (E-Cad) was also found to mark supporting cells and duct/gland cells (Fig. 2D). Although the labeling with these two antibodies was fairly dense in the basal region of the epithelium, careful microscopy demonstrated the staining among the basal cells was due to the density of supporting cell foot processes extending to the basal lamina.

Another set of cytoskeletal proteins that are useful for the typing of nasal cells are the beta-tubulins, which are ubiquitous in the cytoskeleton of all cells but are of variable subtypes. Beta-tubulin, type IV is prominent in cilia<sup>11</sup> and, hence, was tested as a marker useful for distinguishing respiratory epithelial cells from olfactory sustentacular cells. Combining anti-beta-IV with neuronal markers confirms the sharp boundary between these two types of epithelium in humans (Fig. 2E,G). The antibody to beta-IV densely labels the apical surface of respiratory cells and their cilia and is very useful in distinguishing true respiratory epithelium from the degenerative aneuronal olfactory epithelium described previously<sup>2,5,12,13</sup>. As noted above, some cells that closely resemble respiratory or supporting cells are labeled with PGP9.5. Anti-beta-IV antibodies co-label the PGP9.5(+) non-neuronal cells but do not label the PGP9.5(+) neurons (Fig. 2G). This type of non-neuronal labeling with PGP9.5 has been described previously in adults and developing humans<sup>14,15</sup>, and although the dense staining of normal olfactory epithelium in both the sections and whole mounts is clearly neuronal, it is prudent to rule out the staining of respiratory cells with this antibody in areas of degenerated epithelium or where an olfactory identity is uncertain.

**Horizontal basal cells**—The composition of the basal cell population in the human olfactory epithelium has been subject to considerable debate. Morphologically distinct basal cell types can be seen and shown by EM examination, some of which resemble the horizontal basal cells (HBCs) of the rodent olfactory epithelium, while others look more like globose basal cells (GBCs)<sup>16,17</sup>. However, other investigators have suggested that all of the basal cells of the human olfactory epithelium express the cytokeratin proteins that are characteristic of HBCs<sup>7</sup>. A more complete assessment of the basal cell population in human is fundamental to any efforts to evaluate the neurogenic vigor of the epithelium. Thus, the ability to classify basal cells as HBCs or not helps dissect the cellular components of the basal region important in neuronal regeneration. A number of keratin antibodies have been found to label non-neuronal cells of the olfactory epithelium in rodents<sup>17</sup> and humans<sup>7,14</sup>. Antibodies that react with multiple types of keratins (pankeratin) label basal cells in addition to duct/gland and supporting cells (Fig. 3A). These other cell types express K18 (Fig. 2C). In terms of distinguishing HBCs from other cells near the base of the epithelium, antibodies specific to individual types of keratin monomers are more useful than pan-keratin reagents. To that end, we (as well as others<sup>7</sup>) used antibodies to keratin 5 (K5) which appear to be specific to the horizontal basal cells in humans as in rodents (Fig. 3B,E). In our samples, the K5(+) cells form a monolayer that is adherent to the basal lamina, which is precisely the same pattern as described by us in rats and mice<sup>17</sup>. We also expected to find similar staining with antibodies against keratin 14, which is usually paired with keratin 5, but staining with several different antibodies against this protein was unsuccessful (not shown). However

antibodies against keratin 17 (K17) also labeled a monolayer of cells at the basal lamina, as anti-K5 does, i.e. HBCs (Fig. 3C). Simultaneous staining with the two antibodies showed exclusive co-labeling in the epithelium (not shown).

In addition to the keratins, antibodies to the transcription factor p63, which is required for the differentiation of keratin-expressing basal cells in multiple epithelia<sup>18</sup> is also a selective and specific marker for HBCs in the human OE as well as in rodents (Fig. 3D, J), and the p63 labeling is coextensive with that for K5 (Fig. 3F). Staining with other antibodies was found to be less exclusive to HBCs. As seen previously in rodent tissue<sup>17</sup>, antibodies against epidermal growth factor receptor (EGFr) label HBCs as well as supporting cells (Fig 3G). Antibodies to transcription factors Pax6 and Sox2 label nuclei of HBCs but also label supporting cell nuclei (Figs. 3H, I, K). Pax6 also marks duct and gland cells, which do not stain with Sox2 antibodies. With respect to Sox2, some of the Sox2(+) basal cells sit just superficial to the monolayer of HBCs defined by p63. These Sox2(+)/p63(-) basal cells most likely correspond to globose basal cells by analogy to their expression in rodents (Figs. 3K, L).

**Olfactory neurons**—The olfactory sensory neurons, of course, are the cells that give the olfactory epithelium its neural character and subserve its sensory function. Our ability not only to identify these neurons but also categorize them into mature and immature populations provides useful information on the status of the epithelium and its connection with the olfactory bulb. OMP marks the cell bodies, dendrites, and axons of mature olfactory neurons in the human epithelium (Figs. 4A, E). OMP(+) neurons are concentrated in the more apical reaches of the epithelium, but are not as tightly packed, closely ordered and segregated superficially as they are in rodents. Neuron-specific beta-tubulin type III labeling is prominent in neurons, and the monoclonal antibody to this protein (Tuj-1) labels the cell bodies, dendrites and axons of all neurons of the epithelium including mature as well as immature ones (Fig. 4B). Antibodies to the olfactory receptor-specific G-protein ( $G_{olf}$ ) also label mature olfactory neurons and some immature neurons (Fig. 4C) but the staining of dendrites and cell bodies is more intense than that of axons, as compared with OMP, Tuj-1, PGP9.5, or NCAM (Fig. 4 and NCAM, not shown).

The combination of neuron specific antibodies provides useful information on the status of the neuronal population of the OE as a whole. As an example, co-labeling with PGP9.5 and OMP can be used to define PGP9.5(+)/OMP(+) mature neurons and PGP9.5(+)/OMP(-) immature neurons (Figs. 4D, E, F). By comparison to the scant population of mature olfactory neurons illustrated above (Fig. 1), sections of other autopsy specimens provide a much “healthier” appearance in which the population of OMP(+) mature neurons is much more abundant and found superficial to the more basally positioned PGP(+)/OMP(-) immature neurons, e.g., the sample obtained from an 82-year old female with congestive heart failure (Fig. 4F). Given the known association of anosmia with aging<sup>19</sup>, we were surprised to find examples of “healthy-looking” olfactory epithelium containing mature and immature neurons, in specimens including our most elderly subject (age 96) although evidence of patchy respiratory replacement was more extensive in this individual than in others of the group.

**Globose basal cells and progenitor cells**—In rodents, the identification and molecular profile of the globose basal cell (GBC) population is less well developed and is appreciably more complex than the other cell types of the OE. The same appears to be true of humans. Neuronal markers can be combined with HBC-specific antibodies to define a population of GBCs by intercalation and exclusion. Thus, combining PGP9.5 with K5 reveals a population of unstained basal cells situated just apical to the HBCs (Fig 4I). The position of these cells and lack of neuronal/HBC staining match the characteristics of GBCs

in rodents and reinforce their identification as Sox2(+)/p63(-) cells. Furthermore, the surprising utility of transcription factor antibodies allow us to characterize and potentially subdivide further the population of GBCs and their contribution to epithelial regeneration. The achaete-scute homolog 1 transcription factor (Ascl1 or Hash1) is thought to play a significant role in the development of the olfactory neuronal lineage which parallels selected other cell types elsewhere in the CNS or PNS<sup>20,21</sup>. Staining of olfactory mucosa with antibodies against this protein (Mash1) marks nuclei of selected basal cells (Figs. 5B, E, H, K). The Mash1(+) cells can be clustered in a spherical grouping or linear row (Fig. 5H). In this specimen obtained from a 49-year old male with brain cancer, the Mash1(+) cells are distinct from cells that express neuronal-marker Tuj-1 (Fig. 5C) or the HBC-marker p63 (Fig. 5F). Many of these Mash1(+) cells reside in the GBC compartment amongst the K5(-)/PGP(-) cells (cf. Figs. 5F, 4I). As expected, many Mash1(+) cells are mitotically active; they do not co-label with an antibody against the cyclin-dependent kinase inhibitor p27 (Figs. 5G, H, I), but many co-label with antibodies against the cell proliferation antigen Ki67 (Fig. 5L). Ki67 also labeled cells without Mash1 staining (Figs. 5J, L).

In addition to staining for Mash1, we observed a unique staining pattern with antibodies against the transmembrane protein Notch1. The Notch1 signaling cascade regulates the choice point between neuronal vs. non-neuronal differentiation of multipotent progenitors in the olfactory epithelium and elsewhere<sup>22-24</sup>. When activated, the intracellular domain is cleaved and translocates through the cytoplasm to the nucleus, and GBCs are diverted to a non-neuronal cell fate. When Notch signaling is inhibited GBCs form neurons. An antibody to both the membrane-associated and intracellular forms of Notch1 labels occasional basal cells within the olfactory epithelium. The Notch1(+) basal cells sit just superficial to the HBC layer, are pyramidal in shape and are almost certainly GBCs as they are in rodents (Figs. 5M, O).

In sum, we have validated a collection of immunoreagents that can be used either individually or in combination to classify all of the various cell types found within the adult human OE (Table II). It is remarkable the extent to which the pattern of differential expression of these markers in humans mimics that which is characteristic of rodents.

### Immunohistochemical analysis of esthesioneuroblastoma

The comprehensive battery of antibodies outlined above allows us to not only analyze the olfactory epithelium in detail, but also provides us with a valuable tool for assessing the cellular composition of other olfactory-related tissues including known pathologic entities. Olfactory- or esthesioneuroblastomas are undifferentiated tumors of neuroectoderm origin ostensibly derived from the olfactory epithelium. We obtained a specimen of Hyams grade II esthesioneuroblastoma from a 44 year-old female. The diagnosis was confirmed by pathologists from the Massachusetts Eye and Ear Infirmary, and their analysis included immunohistochemical demonstration of expression of synaptophysin and chromogranin, and a lack of staining for p63, keratin, CK7, CK20, and HMB-45. S-100 staining marked some tumor cells and other cells that surrounded nests of tumor cells.

Our battery of antibody reagents was used to analyze the composition of the tumor with the aim of clarifying the types of cells within the tumor, and, potentially, the cell type(s) from which it originates. Where there was overlap in reagents, our findings were identical to the pathologic assessment at the Massachusetts Eye and Ear Infirmary. The majority of the tumor was composed of Tuj-1-stained cells (Fig. 6A), consistent with a neuroectodermal origin, and also labeled for NCAM (see Fig. 8E) and PGP9.5 (not shown). However, OMP, the marker for mature olfactory neurons, was absent (Fig. 6B). Cords of K18-expressing cells separated the tumor into nests (Fig. 6C), indicative of sustentacular- or gland/duct-type differentiation. None of the tumor cells stained with K5, the HBC-specific keratin, although

K5(+) basal cells were evident in the attached surface epithelium (Fig. 6D). As reported by the pathologists, anti-p63 did not stain any cells within the tumor but we did find p63(+) basal cells in the surface epithelium in a pattern equivalent to that for K5 labeling (Fig. 6E). The respiratory cell marker beta-tubulin, type IV was also absent from the tumor (Fig. 6F). G<sub>olf</sub>-marked cells were distributed like the other neuronal markers (Fig. 6G). It is worth noting that G<sub>olf</sub>-positivity provides a clear indication of the olfactory origin of this tumor. In addition, Mash1 labeled a large portion of the tumor (Fig. 6H) in keeping with previous reports that esthesioneuroblastomas are characterized by the expression of achaete-scute homolog 1 mRNA<sup>25,26</sup>. Pax6 antibody also labeled a large number of cells in the tumor as well as basal and supporting cells within the surface epithelium (Fig. 6I).

Perhaps the most illuminating analysis of the tumor was afforded by comparing the distribution of the transcription factors Sox9 and Sox2. Sox9 antibodies, which typically label Bowman's duct/gland cells in the olfactory epithelium of both humans and rodents, mark a majority of the tumor cells; the Sox9(+) cells are arranged in nests and have very large nuclei (Figs. 7B, D, G). When the tumor was double-stained with both the Sox2 and the Sox9 antibodies, two separate populations were observed. Within the tumor, Sox2 labeled cells with smaller nuclei that were often arranged in cords surrounding the nests of Sox9(+) cells (Figs. 7A, C). There was no evidence that tumor cells could be labeled with both.

The two cellular territories were characterized further by a set of double labeling studies. K18 labeling very closely resembled the pattern observed with Sox2; for example, the K18(+) cells surrounded the nests of Sox9(+) cells, but did not label with the Sox9 antibody (Fig. 7F). In contrast, TuJ-1 labeling, i.e., the canonical antibody for demonstrating neuron-specific tubulin, is coextensive with Sox9 throughout the nests of cells (Fig. 7I); only rarely if ever was a cell Sox9(+) and Tuj-1(-). The separation into two distinct territories within the tumor was confirmed by comparing the labeling for K18 and the staining with TuJ-1 (Fig. 8C); no double labeling was observed.

E-cadherin labeling was characteristic of both kinds of territories. For convenience, NCAM was used to define the two distinct territories for comparison with E-cadherin; as cells were uniformly TuJ-1(+)/NCAM(+) (not shown), or stained by neither reagent, the presence of NCAM can be taken as indicative of the Sox9 nests. When the tumor was stained for both NCAM and E-cadherin, it was evident that E-cadherin labeled both the nests of Sox9(+)/TuJ-1(+)/NCAM(+) large cells and the surrounding cords of Sox2(+)/K18(+) small cells (Figs. 8D, F). Since E-cadherin is expressed by both supporting cells and gland/duct cells in the olfactory epithelium, labeling of both regions of the tumor was not a surprise.

Finally, we assayed the tumor for the expression of another human HBC marker that we identified, namely K17, which mirrors the labeling of olfactory epithelium with K5 very closely. However, in the case of the esthesioneuroblastoma tissue, K17, but not K5, labeled cells in a small patch of the tumor (Fig. 9A and inset). In contrast, K17 and K5 were co-extensive in staining the HBCs in the pieces of normal epithelium lining the surface of the tumor (not shown). Within the invasive tumor tissue, a few sporadic K17(+) cells were also labeled by the neuronal marker Tuj-1 (Fig. 9C).

## Discussion

With recent advances in understanding the development and regeneration of olfactory epithelium in rodents, we are potentially in a better position to assess the pathological changes in the human olfactory epithelium that are responsible for olfactory loss. However, for an accurate translation from experimental models of injury and repair to human

pathophysiology we first need to establish the overall similarity of molecular phenotypes between rodents and humans by immunohistochemical or other means.

We approached the analysis of the human olfactory mucosa on two levels. First, we developed a protocol for the macroscopic assessment of the distribution of olfactory mucosa (OM) within the nasal cavity. Second, we applied our panel of cell type-specific markers, developed for use in rodents, to an in-depth analysis of the composition of the human tissue. With regard to the former, the upper nasal mucosa retains considerable areas of neuroepithelium even in the most elderly individuals. The extent of the olfactory epithelium and the borders of the olfactory area were variable across cases, but invariably included the area directly inferior to the cribriform plate, and often extended to the face of the sphenoid. Intervening patches of respiratory epithelium were common as described previously<sup>1</sup>. Although olfactory epithelium has been reported as far anterior as the anterior attachment of the middle turbinate<sup>27</sup>, that was not the case in our specimens where the OM was more limited; which may reflect the advanced age of our cases since the human OM may be much more extensive at birth<sup>1</sup>. The analysis of the distribution of OM by whole mount (WM) may also provide further insight into the relationship of olfaction to age and disease.

Regardless of the full extent of OM in the nasal cavity, the dense concentration of olfactory neurons in the area directly beneath the cribriform plate is a consistent feature even in the elderly. For purposes of OM biopsies, the cleft is a difficult area to access, and the reported suboptimal rate for obtaining true olfactory epithelium likely reflects that inaccessibility<sup>4</sup>. A large portion of the mucosa lining the middle and superior turbinates was also analyzed. Substantial parts of the mucosa on the lateral wall contained neuroepithelium, however, the olfactory area of the septum was more extensive and was characterized by a lesser degree of respiratory replacement. With these findings in mind, opportunities for successful harvest of OM are maximal when directing biopsies to the region of septal epithelium directly below the cribriform plate.

Material harvested at autopsy also provides an advantage for immunohistological assessment of the cellular composition of the OM. The full-thickness strip harvested from the septum has the advantage of size, which imparts a more integrated view of the mucosa and includes epithelium rich in olfactory neurons, as verified by whole mount staining. In addition, the sample can be oriented properly for sectioning more easily than biopsies, which is crucial for assessing arrangement of the cells in the epithelium and the prominence of the various cell populations, including HBCs, which normally form a monolayer but can accumulate to a greater number and depth after epithelial injury.

The results of our immunohistochemical analysis of cell types and their prevalence in the human OM are essentially identical in broad strokes and in detail to findings in the OM of experimental animals and are mostly consistent with previous analyses in human tissue harvested at autopsy or by biopsy. In particular, antibodies against several key transcription factors and signal cascades involved in the assembly of the OE in rodents are also informative when applied to the human epithelium.

For example, the status of the basal cell population is of key import to the regenerative capacity of the olfactory epithelium in experimental animals. In addition to the stem and progenitor cell activity within the population of GBCs, the HBC population has been recently identified in mice as an additional reserve stem cell population that can be activated by injury<sup>28</sup>. Our analysis has clarified the status of these two populations in the human olfactory epithelium. Suggestions that all of the basal cells of the olfactory epithelium are keratin-expressing and HBC-like are not supported by our data<sup>7</sup>. We find a distinct monolayer of HBCs, labeled by the usual markers – K5, EGF-R, p63, Pax6, and Sox2.

Situated superficial to the layer of HBCs are cells that have the characteristics of GBCs – marked by Mash1, Sox2, Pax6, Notch1, and Ki-67 (the latter indicating a high rate of mitotic activity) – without expressing K5, K17, or K18. We cannot explain the discrepancy with prior reports in full, however, it should be noted that when staining sections for HBCs and other epithelial components, we confirmed the tissue as OE and not respiratory epithelium with double labeling using anti-neuronal antibodies on the same section (Fig. 4I) or near adjacent sections. Squamous metaplasia with multiple layers of keratin(+) cells has been described in human OE samples and has been associated with chronic rhinosinusitis<sup>8</sup>. In these conditions the epithelium is abnormal. Based on our observations using sections of OE with confirmed olfactory neurons, a basal monolayer of CK5(+)/p63(+) HBCs is the norm with a more superficial, separate population of GBCs.

In addition to clarifying the basal cell population, the use of these reagents has also suggested that the various cell types differentiate from their progenitors in a manner similar to that revealed in experimental animals. Thus, the expression of the basic helix-loop-helix transcription factor Hes1 (the canonical downstream effector of Notch signaling) in sustentacular (Sus) cells, and the expression of Notch1 by GBCs is precisely the same as in rodents. In them, manipulating gene expression has shown that Notch1 activation diverts GBCs toward the formation of Sus cells during the regeneration of the injured olfactory epithelium (unpublished results), presumably by blocking the expression of Mash1, which is required for progenitors to advance to the generation of neurons. Likewise, the selective expression of Sox9 by duct/gland cells and Sox2 by Sus cells in partnership with Pax6 in both cell types, is seen in human olfactory epithelium as in rodents, where the switch from Sox9 to Sox2 accompanies the differentiation of Sus cells from residual duct/gland cells during epithelial regeneration.

Of course, the other feature that defines the overall "health" of the mucosa is the status of the neuronal population of the epithelium, which has been assessed in the past (by ourselves and others) by the extent of staining with various neuronal markers. The olfactory epithelium can be aneuronal (but distinguished from respiratory by labeling of the latter with beta-tubulin, type IV) or the neuronal population can vary in size and the relative proportion of immature vs. mature olfactory neurons (as determined by the number of neurons that are marked by TuJ-1 alone or by both TuJ-1 and OMP, respectively). The presence of any immature neurons is an indirect, but powerful indication that neurogenesis is carrying on, even in patients as old as these. However, the population of mature neurons should be larger than that of immature ones, and is generally found to be so when the epithelium is thick and neurons are numerous. A high ratio of immature to mature neurons suggests either a recent insult to the epithelium requiring neuronal replacement, or an inability of mature neurons to connect with the olfactory bulb for whatever reason--known (for example, due to head trauma or other forms of damage to the bulb itself) or unknown. On the other hand, scant numbers of both mature and immature neurons may be due to a dwindling of the neurogenic capacity as stem and progenitor cells become exhausted by ongoing damage to the epithelium itself or permanent interruption of the axonal pathway to the bulb. A fuller view of the neurogenic capacity of the epithelium must take the status of the GBC population into account. We show here that labeling for Mash1 (the neurogenic basic helix-loop-helix transcription factor) and Ki-67 (characteristic of proliferating cells) provides an estimate, albeit incomplete, of that capacity. Mash1, which is labeling only GBCs and not marker-identified neurons or HBCs, marks cells in clusters or layered groups that are mitotically active. Given that neurogenesis cannot proceed in the absence of functional Mash1 in rodents<sup>20,21,29</sup>, and that the phenotype of the Mash1-labeled cells in the human is similar, the status of the Mash1 population may provide a way of distinguishing between progenitor cell exhaustion vs. ongoing regeneration in those case where the neurons are few and immature ones predominant in the setting of clinical olfactory loss.

The potential usefulness of our immunohistochemical panel and approach is also exemplified by the analysis of olfactory epithelial-derived tissue such as esthesioneuroblastomas. These tumors are thought to be of neuroectodermal origin and their derivation from olfactory epithelium is assumed on the basis of their common association with the cribriform area, staining characteristics, and finding of Mash1 mRNA expression within the tumor<sup>25,26</sup>. These tumors may present with varying degrees of differentiation and are sometimes difficult to diagnose from other undifferentiated sinonasal tumors such as sinonasal undifferentiated carcinoma and lymphoma. In these settings, definitive antibody labeling characteristics may be helpful in determining the pathology.

Overall the immunostaining in our case confirmed the analysis performed by the clinical pathologists – keratins and p63 were absent, but neurogenic markers stained strongly. Labeling of presumed esthesioneuroblastomas with p63 antibodies has been reported in the literature<sup>30</sup>, however the absence of this marker remains a common criterion for identifying lesions as esthesioneuroblastomas – a criterion satisfied by the case presented here. The controversy regarding the expression of p63 in esthesioneuroblastomas may derive, in part, from difficulties in determining what cells are or aren't part of the tumor, particularly since we see p63(+) HBCs in the remnants of normal epithelium that overrides the invasive mass. That the tumor labeled with G<sub>olf</sub> antibodies also provides convincing evidence of its olfactory epithelial origin. Although this G-protein has been found in other areas of the body including the testis, retina, basal ganglia, liver, and pancreatic islet cells<sup>31</sup>, it is the G-protein associated with signal transduction in olfactory neurons<sup>32</sup> and is not found in other nasal tissue. In addition to G<sub>olf</sub> staining, our findings of extensive antibody labeling with Mash1 are a honed extension of prior mRNA studies<sup>25,26</sup> and further support the association with olfactory epithelium. The combined use of these markers may prove beneficial in the diagnosis of undifferentiated masses of the nasal cavity.

Most strikingly, we were able to subdivide the tumor into two major cell types and regions using other markers from our panel. One type of tumor cell is strongly labeled with K18 and Sox2 antibodies reminiscent of Sus cells or other non-neuronal epithelia, and the other is labeled with neuronal markers such as Tuj-1 and NCAM, as well as Sox9. The latter was a surprising and intriguing finding, since Sox9 is limited to the Bowman's gland and duct cells of the OE (which also do not express Sox2), and does not cross-over to neurons in normal tissue. E-Cadherin staining was common to both regions of the tumor and is expressed by both duct/gland cells and supporting cells in the normal epithelium. These findings suggest a glandular component to the Sox9/neuronal portion of the tumor and a distinct pathway toward differentiation of the surrounding K18/Sox2(+) sustentacular-like cells. It is worth noting that both GBCs and HBCs can give rise to duct/gland cells during the regeneration of injured epithelium<sup>10,28</sup>. Indeed, transplanted GBCs give rise to only neurons and duct/gland cells on occasion<sup>10</sup>. Thus, the Sox9/neuronal tumor cells may resemble that set of GBCs responsible for that result. Alternatively, the cellular phenotype may reflect a capacity of Bowman's gland and/or duct cells to serve as stem or progenitor cells during epithelial regeneration, as has been suggested previously<sup>33</sup>. Cells expressing Sox9 in other epithelia such as the epidermis have been associated with stemness; there, the Sox9-expressing cells occupy a specific niche of the hair follicle and give rise to all epidermal lineages<sup>34</sup>. Sox9 expressing cells within the Bowman's glands may be playing a similar role in the OE, and also may be a potential source for mutagenesis and development of esthesioneuroblastomas.

We are now in a position to analyze the human olfactory epithelium in depth and in detail by application of a panel of immunohistochemical reagents with additional emphasis on cell lineage markers. By this approach we can discern the dynamic state of the epithelium and correlate pathological findings with clinical olfactory ability with more assurance. Further studies of human olfactory biopsies will be needed to elucidate the pathophysiology of

olfactory disorders further. Moreover, additional investigations of olfactory pathology, for example as shown by the study of esthesioneuroblastoma, may also lend insight into the regenerative processes of the olfactory epithelium, as well as tumorigenesis.

## Conclusion

Human olfactory mucosa is very similar to rodents with respect to the molecular phenotypes of its constituent cells. Multiple transcription factors known to be crucial in the development and maintenance of the olfactory epithelium are found in human olfactory mucosa and provide a valuable tool for the assessing the regenerative state and the neurogenic capacity of the epithelium. Accordingly, a detailed immunohistochemical characterization of this type can be helpful not only in understanding the pathophysiology of olfactory disorders but may also help elucidate the origin of esthesioneuroblastomas. Nonetheless, further work with these and a rapidly expanding list of antibodies that mark progenitor and stem cells will be needed to advance our understanding olfactory dysfunction in humans.

## Acknowledgments

This work was funded in part from the NIH/NIDCD (R01DC010242) and a generous donation from Mr. David Clem. Technical advice in preparing this manuscript from Dr. Woonchan Jang, Dr. Adam Packard, Dr. Richard Krowlowski, and Nikolai Schnittke is greatly appreciated.

## References

1. Naessen R. The identification and topographical localisation of the olfactory epithelium in man and other mammals. *Acta Otolaryngol.* 1970; 70:51–57. [PubMed: 4917513]
2. Nakashima T, Kimmelman CP, Snow JB Jr. Structure of human fetal and adult olfactory neuroepithelium. *Arch Otolaryngol.* 1984; 110:641–646. [PubMed: 6477257]
3. Paik SI, Lehman MN, Seiden AM, Duncan HJ, Smith DV. Human olfactory biopsy. The influence of age and receptor distribution. *Arch Otolaryngol Head Neck Surg.* 1992; 118:731–738. [PubMed: 1627295]
4. Hasegawa S, Yamagishi M, Nakano Y. Microscopic studies of human olfactory epithelia following traumatic anosmia. *Arch Otorhinolaryngol.* 1986; 243:112–116. [PubMed: 3718322]
5. Holbrook EH, Leopold DA, Schwob JE. Abnormalities of axon growth in human olfactory mucosa. *Laryngoscope.* 2005; 115:2144–2154. [PubMed: 16369158]
6. Feng WH, Kauer JS, Adelman L, Talamo BR. New structure, the "olfactory pit," in human olfactory mucosa. *Journal of Comparative Neurology.* 1997; 378:443–453. [PubMed: 9034902]
7. Hahn CG, Han LY, Rawson NE, et al. In vivo and in vitro neurogenesis in human olfactory epithelium. *J Comp Neurol.* 2005; 483:154–163. [PubMed: 15678478]
8. Yee KK, Pribitkin EA, Cowart BJ, et al. Neuropathology of the olfactory mucosa in chronic rhinosinusitis. *Am J Rhinol Allergy.* 2010; 24:110–120. [PubMed: 20021743]
9. Huard JM, Youngentob SL, Goldstein BJ, Luskin MB, Schwob JE. Adult olfactory epithelium contains multipotent progenitors that give rise to neurons and non-neural cells. *J Comp Neurol.* 1998; 400:469–486. [PubMed: 9786409]
10. Chen X, Fang H, Schwob JE. Multipotency of purified, transplanted globose basal cells in olfactory epithelium. *J Comp Neurol.* 2004; 469:457–474. [PubMed: 14755529]
11. Roach MC, Boucher VL, Walss C, Ravdin PM, Luduena RF. Preparation of a monoclonal antibody specific for the class I isotype of beta-tubulin: the beta isotypes of tubulin differ in their cellular distributions within human tissues. *Cell Motility & the Cytoskeleton.* 1998; 39:273–285. [PubMed: 9580378]
12. Holbrook EL, Leopold D, Schwob JE. A description of axonal abnormalities observed in human olfactory epithelium. *Chem Senses.* 2003; 28 in press.

13. Yamagishi M, Fujiwara M, Nakamura H. Olfactory mucosal findings and clinical course in patients with olfactory disorders following upper respiratory viral infection. *Rhinology*. 1994; 32:113–118. [PubMed: 7530857]
14. Witt M, Bormann K, Gudziol V, et al. Biopsies of olfactory epithelium in patients with Parkinson's disease. *Movement Disorders*. 2009; 24:906–914. [PubMed: 19205070]
15. Johnson EW, Eller PM, Jafek BW. Protein gene product 9.5-like and calbindin-like immunoreactivity in the nasal respiratory mucosa of perinatal humans. *Anat Rec*. 1997; 247:38–45. [PubMed: 8986301]
16. Graziadei PP, Monti Graziadei GA. Neurogenesis and neuron regeneration in the olfactory system of mammals. I. Morphological aspects of differentiation and structural organization of the olfactory sensory neurons. *J Neurocytol*. 1979; 8:1–18. [PubMed: 438867]
17. Holbrook EH, Szumowski KE, Schwob JE. An immunochemical, ultrastructural, and developmental characterization of the horizontal basal cells of rat olfactory epithelium. *J Comp Neurol*. 1995; 363:129–146. [PubMed: 8682932]
18. Crum CP, McKeon FD. p63 in epithelial survival, germ cell surveillance, and neoplasia. *Annu Rev Pathol*. 2010; 5:349–371. [PubMed: 20078223]
19. Doty RL. Influence of age and age-related diseases on olfactory function. *Ann N Y Acad Sci*. 1989; 561:76–86. [PubMed: 2525363]
20. Cau E, Gradwohl G, Fode C, Guillemot F. Mash1 activates a cascade of bHLH regulators in olfactory neuron progenitors. *Development*. 1997; 124:1611–1621. [PubMed: 9108377]
21. Cau E, Casarosa S, Guillemot F. Mash1 and Ngn1 control distinct steps of determination and differentiation in the olfactory sensory neuron lineage. *Development*. 2002; 129:1871–1880. [PubMed: 11934853]
22. Lindsell CE, Boulter J, diSibio G, Gossler A, Weinmaster G. Expression patterns of Jagged, Delta1, Notch1, Notch2, and Notch3 genes identify ligand-receptor pairs that may function in neural development. *Mol Cell Neurosci*. 1996; 8:14–27. [PubMed: 8923452]
23. Schwarting GA, Gridley T, Henion TR. Notch1 expression and ligand interactions in progenitor cells of the mouse olfactory epithelium. *J Mol Histol*. 2007; 38:543–553. [PubMed: 17605079]
24. Manglapus GL, Youngentob SL, Schwob JE. Expression patterns of basic helix-loop-helix transcription factors define subsets of olfactory progenitor cells. *J Comp Neurol*. 2004; 479:216–233. [PubMed: 15452857]
25. Carney ME, O'Reilly RC, Sholevar B, et al. Expression of the human Achaete-scute 1 gene in olfactory neuroblastoma (esthesioneuroblastoma). *J Neurooncol*. 1995; 26:35–43. [PubMed: 8583243]
26. Mhawech P, Berczy M, Assaly M, et al. Human achaete-scute homologue (hASH1) mRNA level as a diagnostic marker to distinguish esthesioneuroblastoma from poorly differentiated tumors arising in the sinonasal tract. *Am J Clin Pathol*. 2004; 122:100–105. [PubMed: 15272537]
27. Leopold DA, Hummel T, Schwob JE, Hong SC, Knecht M, Kobal G. Anterior distribution of human olfactory epithelium. *Laryngoscope*. 2000; 110:417–421. [PubMed: 10718430]
28. Leung CT, Coulombe PA, Reed RR. Contribution of olfactory neural stem cells to tissue maintenance and regeneration. *Nat Neurosci*. 2007; 10:720–726. [PubMed: 17468753]
29. Caggiano M, Kauer JS, Hunter DD. Globose basal cells are neuronal progenitors in the olfactory epithelium: a lineage analysis using a replication-incompetent retrovirus. *Neuron*. 1994; 13:339–352. [PubMed: 8060615]
30. Bourne TD, Bellizzi AM, Stelow EB, et al. p63 Expression in olfactory neuroblastoma and other small cell tumors of the sinonasal tract. *Am J Clin Pathol*. 2008; 130:213–218. [PubMed: 18628089]
31. Zigman JM, Westermark GT, LaMendola J, Boel E, Steiner DF. Human G(olf) alpha: complementary deoxyribonucleic acid structure and expression in pancreatic islets and other tissues outside the olfactory neuroepithelium and central nervous system. *Endocrinology*. 1993; 133:2508–2514. [PubMed: 8243272]
32. Jones DT, Reed RR. Golf: an olfactory neuron specific-G protein involved in odorant signal transduction. *Science*. 1989; 244:790–795. [PubMed: 2499043]

33. Matulionis DH. Ultrastructural study of mouse olfactory epithelium following destruction by ZnSO<sub>4</sub> and its subsequent regeneration. *Am J Anat.* 1975; 142:67–89. [PubMed: 1121958]
34. Nowak JA, Polak L, Pasolli HA, Fuchs E. Hair follicle stem cells are specified and function in early skin morphogenesis. *Cell Stem Cell.* 2008; 3:33–43. [PubMed: 18593557]

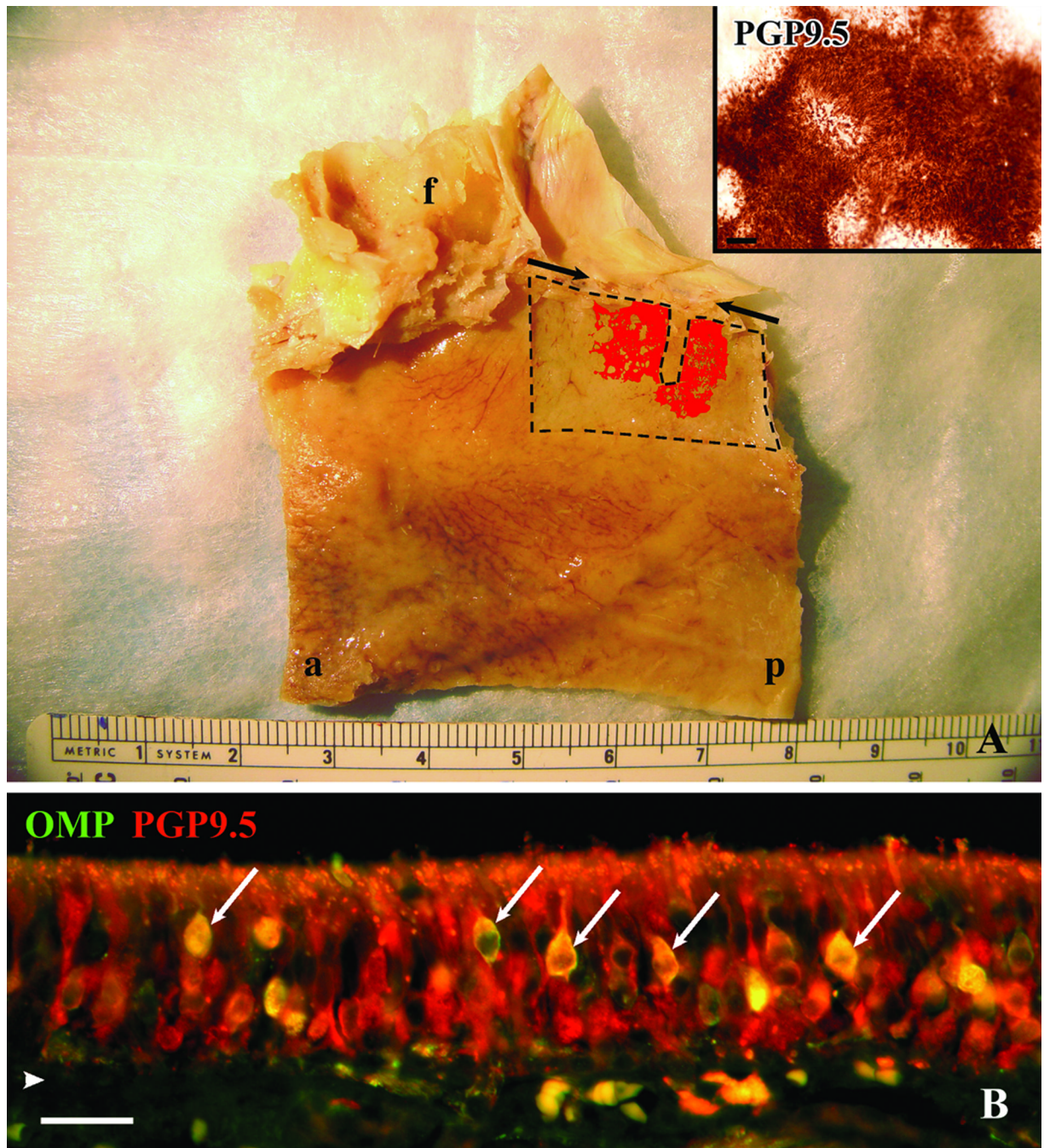


**Figure 1.**

Autopsy specimens provide tissue for both a comprehensive perspective of the extent of neuronal staining and a detailed characterization of olfactory mucosa. **A.** Whole mount staining of the left septum taken from a 75 year-old male with Alzheimer's. The edges of the whole mount stripped from the underlying bone are delineated by **dashed lines**. The thin rectangular defect extending from the superior boarder corresponds to the region removed from the whole mount for histology. The pattern of PGP9.5 staining of the mucosal whole mount is represented in **red** and is superimposed on a photograph taken of the septum after removal of the mucosa. The **inset** is a higher power magnification of the actual PGP9.5 staining at the surface of the whole mount. Notice the circular patches of non-neuronal

epithelium at the edges of the olfactory boarder and within the olfactory region seen in the whole mount representation and inset. **Arrows** indicate anterior and posterior extent of the cribriform plate, **f** = frontal sinus, **a** = anterior, **p** = posterior, **scale bar** = 50 $\mu$ . **B.** Section of epithelium from specimen shown in (A) fluorescently double labeled with OMP and PGP9.5 antibodies. PGP9.5 labels mature and immature olfactory neurons and OMP labels only the mature neurons. In this specimen the double labeled mature neurons (**arrows**) are relatively few compared to the abundant PGP9.5(+)/OMP(-) immature neurons. **arrowhead** = basement membrane, **scale bar** = 25 $\mu$ .

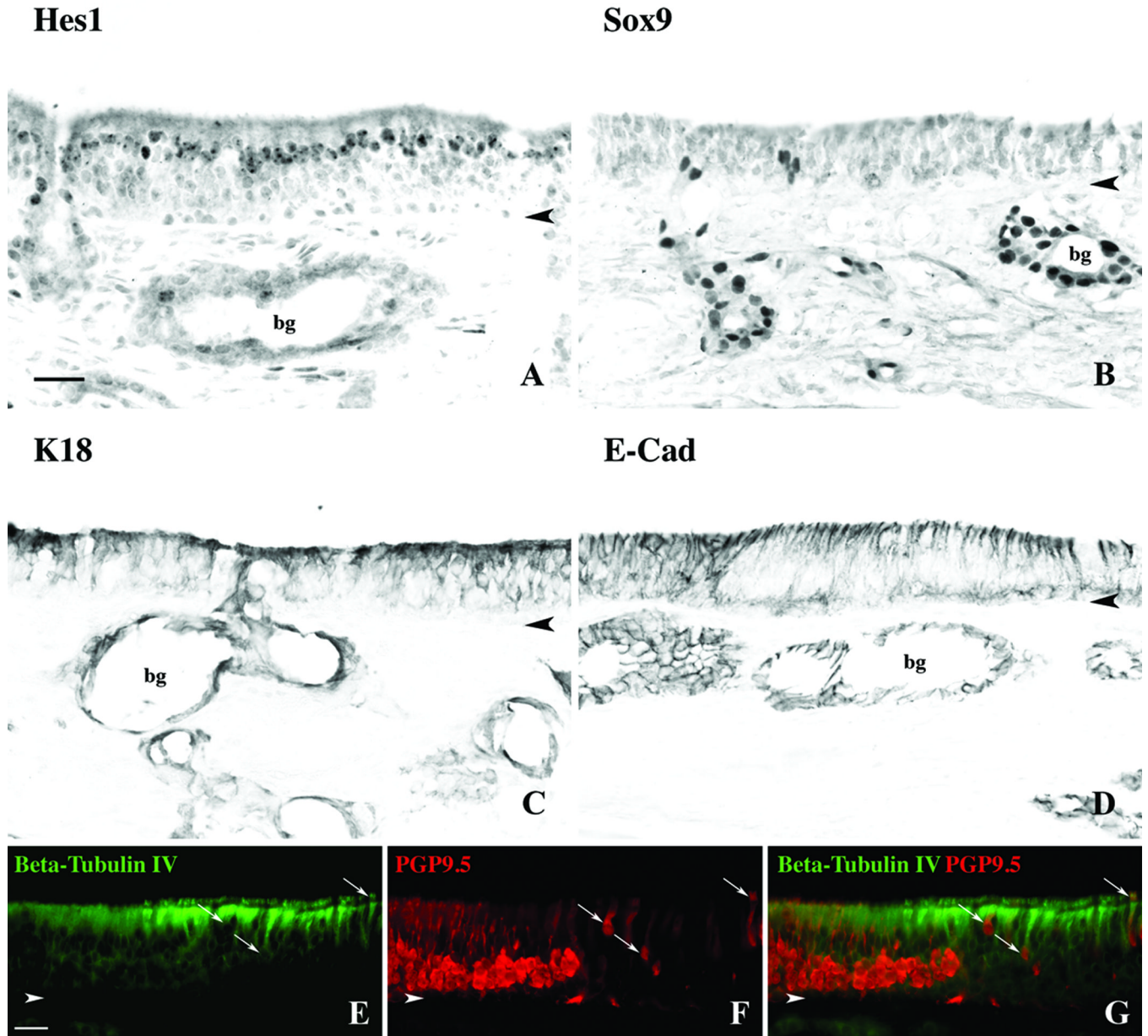


**Figure 2.** Non-neuronal components of the OE can be identified with various antibodies. **A.** DAB staining with the antibody to the transcription factor Hes1 labels nuclei of the supporting cells. **B.** The antibody to transcription factor Sox9 labels duct/gland cell nuclei only. **C.** Antibodies to K18 label both sustentacular cells as well duct/gland cells. **D.** Antibodies to E-Cadherin stain with a similar pattern to K18. **E,F,G.** Double immunofluorescent labeling of a sharp transitional zone between olfactory and respiratory epithelium with antibodies to Beta-tubulin IV and PGP9.5. Beta-tubulin IV densely labels the apical portion and cilia of the respiratory cells. Within the OE, PGP9.5 labels the cell body, axons and dendrites of the olfactory neurons. Several ciliated cells within the respiratory epithelium are labeled with both antibodies (**arrows**) and are clearly non-neuronal. **Bg** = bowman's glands, **arrowheads** = basement membrane, **scalebar** = 25 $\mu$ .

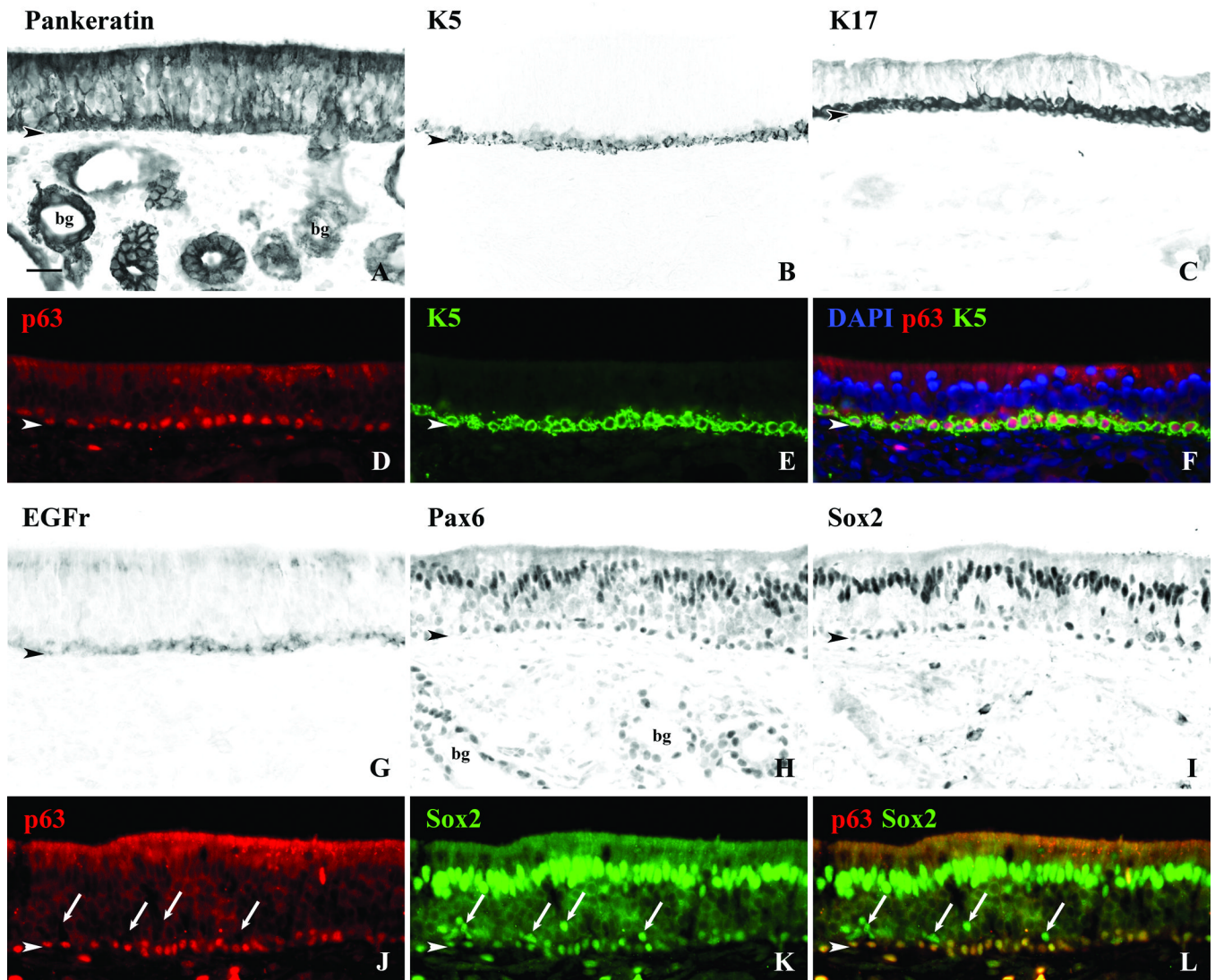


**Figure 3.**

Horizontal basal cells (HBCs) can be identified using multiple antibodies. **A.** DAB staining with the Pankeratin antibody labels HBCs, supporting cells, and Bowman's gland (**bg**) and duct cells. The K5 and K17 antibodies are specific for HBCs in the OE (**B and C**). **D,E,F.** An antibody to the transcription factor, p63, labels nuclei of the HBCs as confirmed with double labeling using the K5 antibody. **G.** DAB staining with antibodies to EGF receptor (EGFr) label HBCs as well as supporting cells to a lesser degree. **H,I.** Staining of adjacent sections with antibodies to transcription factors Pax6 and Sox2 label nuclei of supporting cells and HBCs, but Pax6 also labels duct/gland cells. **J,K,L.** Double immunofluorescent staining of the epithelium with p63 and Sox2 confirms co-labeling of HBCs, but occasional Sox2(+)/p63(-) cells are found just above the HBC layer (**arrows**) and likely correspond to globose basal cells. **bg** = Bowman's glands, **arrowhead** = basement membrane, **scale bar** = 25 $\mu$ .

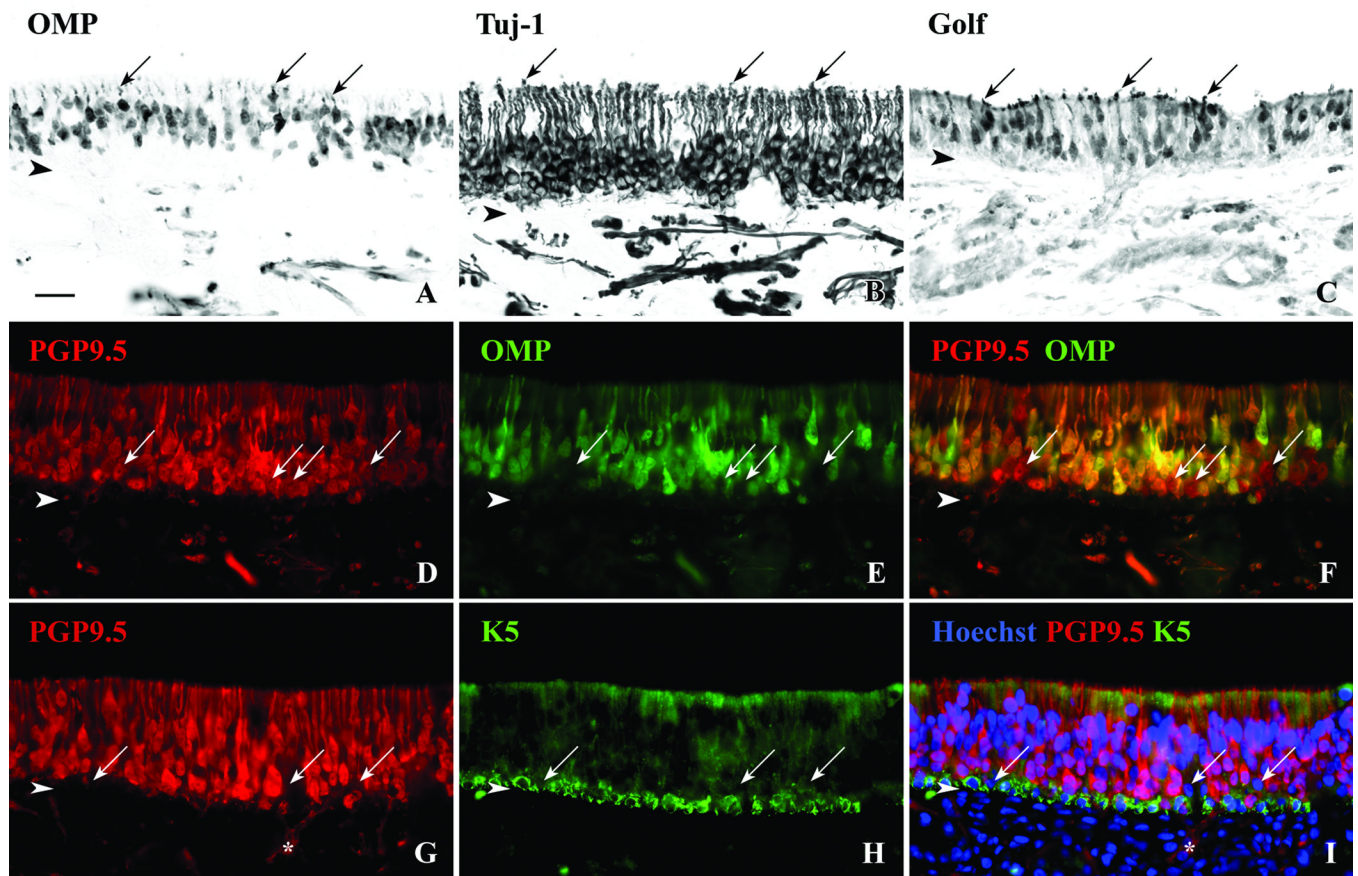


**Figure 4.** Multiple antibodies can be used to identify subpopulations of olfactory neurons (ONs). **A.** DAB staining with OMP antibodies label mature ONs that tend to reside in the more apical portion of the epithelium. **B.** Antibodies to Tuj-1 label both mature and immature ONs with dense labeling of the dendrites and axons. **C.** The antibody to  $G_{olf}$  labels mature and immature ONs with at a higher density in the dendrites and cell bodies. **Arrows** = dendritic knobs. **D,E,F.** Double immunofluorescent labeling of the epithelium with antibodies to PGP9.5 and OMP demonstrates the relative numbers of mature vs. immature ONs. Normal olfactory epithelium contains abundant OMP(+)/PGP9.5(+) mature neurons and OMP(-)/PGP9.5(+) immature neurons (**arrows**) suggesting a dynamic neuroepithelium. **G,H,I.** With double immunofluorescent labeling of the epithelium using HBC marker K5 and ON marker PGP9.5, cells are identified just above the HBCs that are absent of staining for either antibody (**arrows**). These cells may be GBCs or early neuroprogenitor cells. **Asterisk** identifies olfactory nerve fascicles extending out from the basal layer of the epithelium. **Arrowheads** = basement membrane, **scale bar** = 25 $\mu$ .

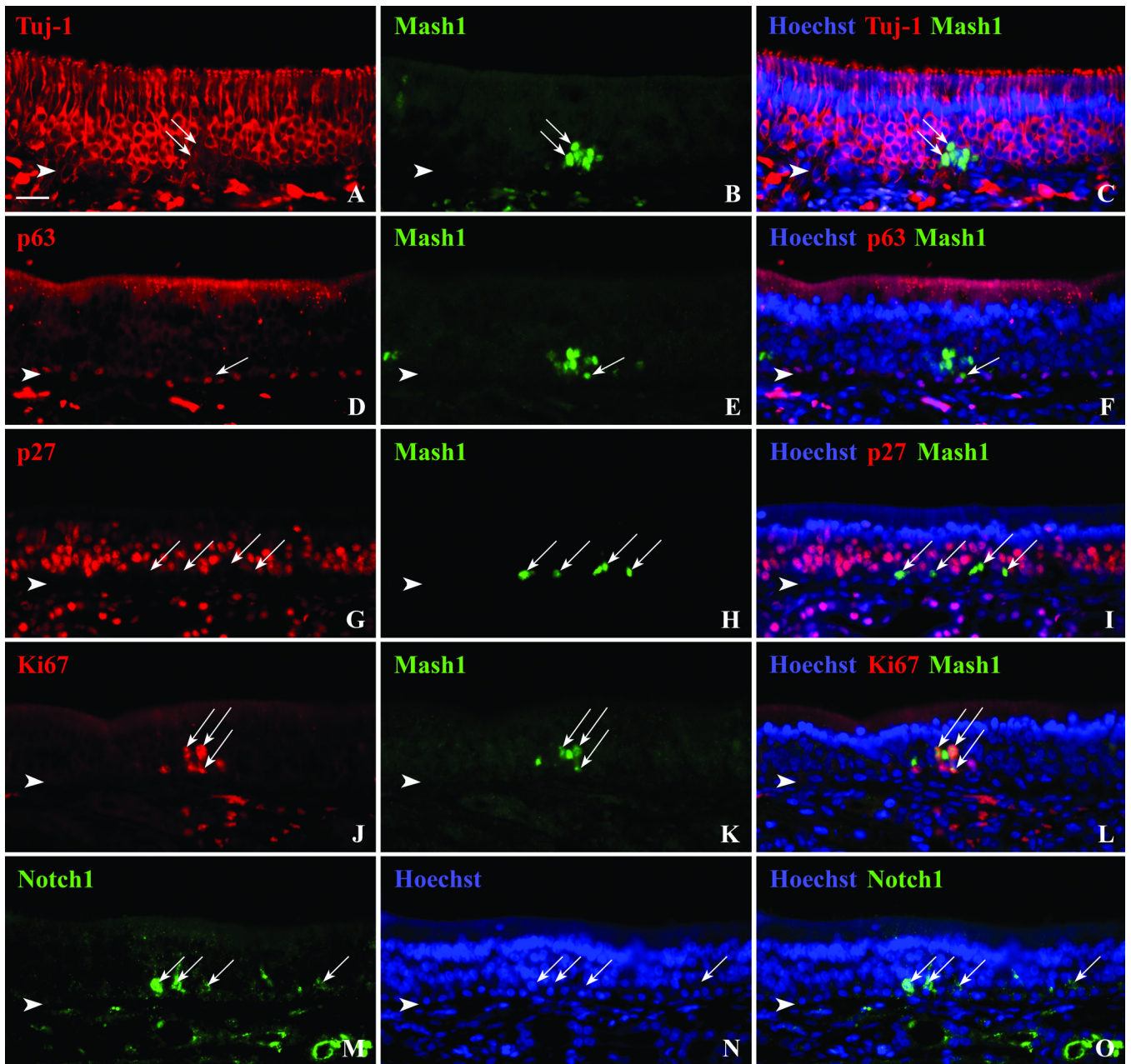


**Figure 5.** Transcription factor antibodies allow us to identify a subset of globose basal cells (GBCs). Immunofluorescent staining with Mash1 antibodies label clusters of cells in the OE (**B,E,H,K**). **A,B,C**. Mash1(+) cells (**arrows**) are not neurons as shown by lack of co-labeling with the anti-neuronal antibody Tuj-1. **D,E,F**. Mash1(+) cells are not HBCs as shown by absence of double staining with p63 antibodies. An **arrow** identifies a Mash1 stained cell sitting just above a p63 stained HBCs in a position typically occupied by GBCs. **G,H,I**. The absence of p27 double labeling with Mash1 (**arrows**) suggests that these cells are not quiescent. **J,K,L**. Many Mash1(+) cells (**arrows**) are mitotically active as shown by double labeling with Ki67 antibodies. **M,N,O**. Notch1 antibodies also label cells within the GBC compartment (**arrows**). **Arrowheads** = basement membrane, **scale bar** = 25 $\mu$ .

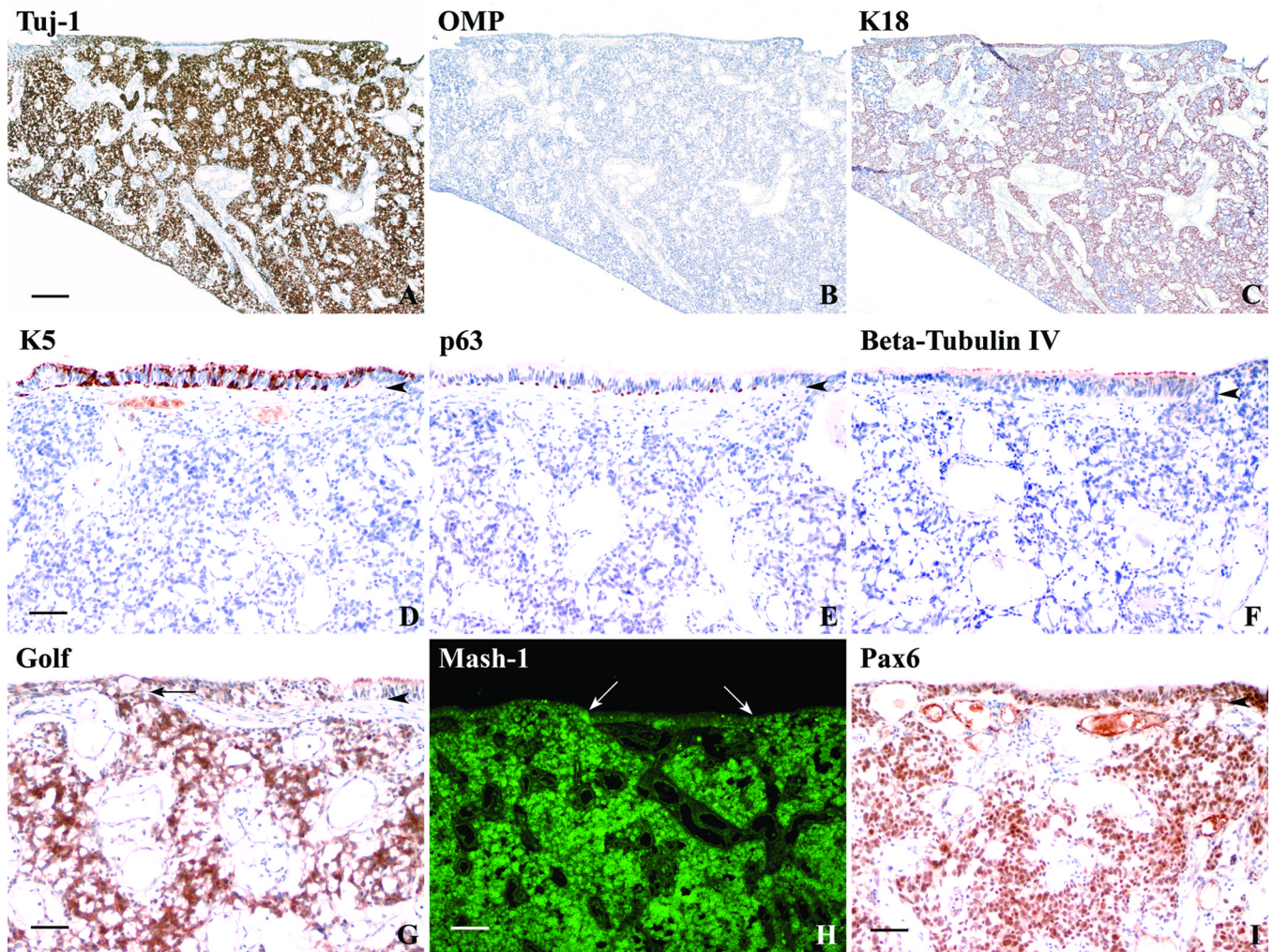


**Figure 6.**

Esthesioneuroblastoma can be characterized using antibody reagents similar to that used for OE. **A.** DAB stained section of a portion of an esthesioneuroblastoma taken from a 44 year-old female using the neuron-specific antibody Tuj-1 labels the majority of the tumor as expected. **B.** However, these cells are not mature ONs based on the absence of OMP staining. **C.** The sustentacular and gland/duct cell specific K18 antibody labels cords of cell separating the tumor into nests. (Scale bar = 250 $\mu$  for **A**, **B**, and **C**.) **D.** The tumor does not stain with antibodies to K5, p63 (**E**), and Beta-Tubulin IV (**F**). Only cells of the epithelial surface overlying the tumor stain with antibodies to K5, p63, and Beta-Tubulin IV indicating a respiratory-like epithelium. (Scale bar = 50 $\mu$  for **D**, **E**, and **F**.) **G.** DAB staining using the  $G_{olf}$  antibody also labels a large portion of the tumor in a pattern similar to Tuj-1 supporting an olfactory epithelial origin of the tumor. An **arrow** indicates extension of the tumor cells into the overlying epithelium (scale bar = 50 $\mu$ ). **H.** Immunofluorescent staining using antibodies to Mash1 also stains a large portion of the tumor in a pattern similar to Tuj-1 and  $G_{olf}$  and corroborates previous mRNA findings. **Arrows** indicate areas of tumor extension into the overlying epithelium (scale bar = 100 $\mu$ ). **I.** DAB staining with Pax6 antibodies labels a large portion of the tumor and the overlying epithelium (scale bar = 50 $\mu$ ). **Arrowheads** = basement membrane.

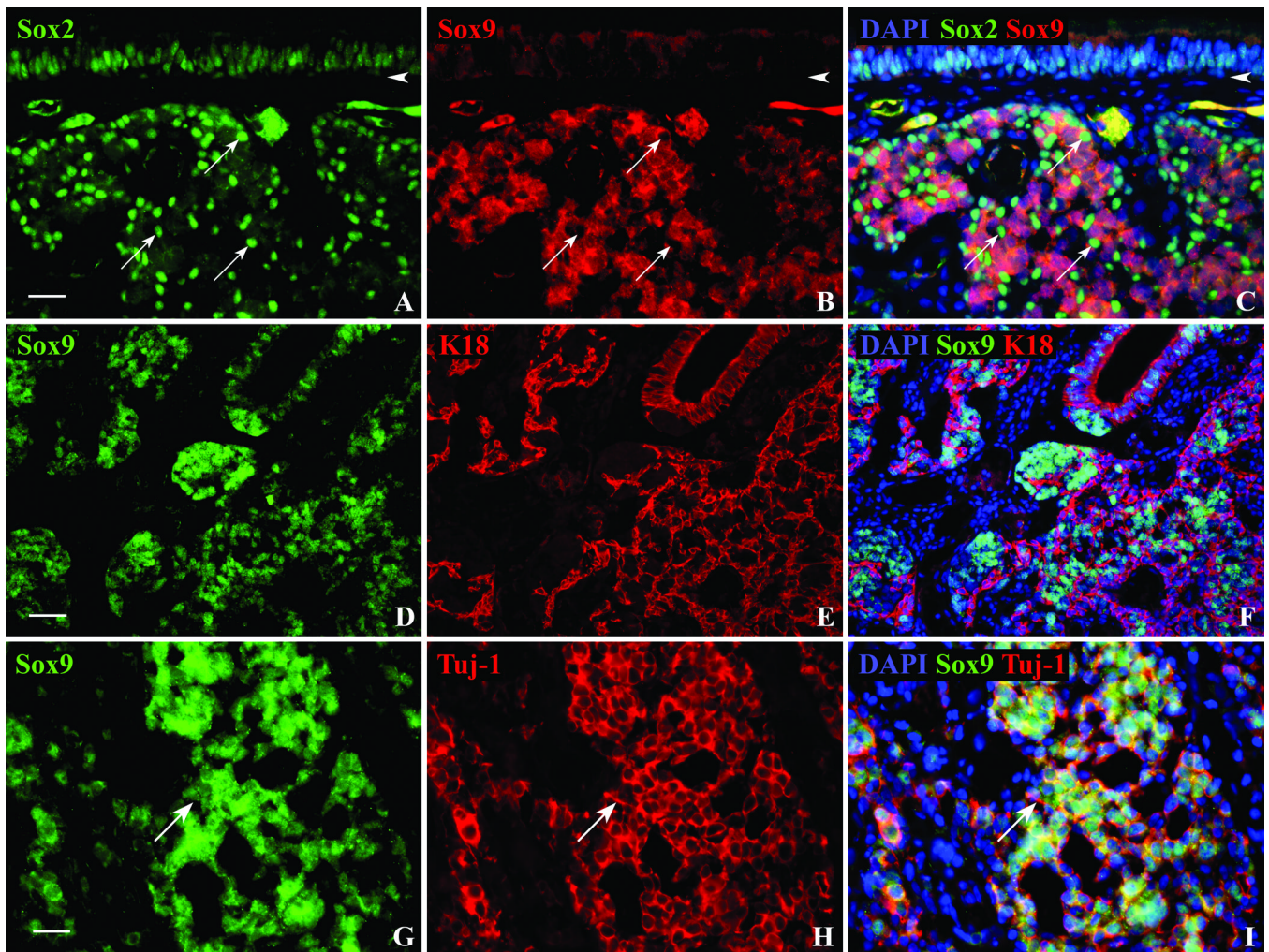


**Figure 7.**

The esthesioneuroblastoma can be divided into two distinct populations using a combination of transcription factor and structural antibodies. **A,B,C.** Double immunofluorescent staining with Sox2 (arrows) and Sox9 antibodies show a mutually exclusive staining pattern within the tumor. Sox2(+) nuclei seem to occur at the periphery of the Sox9(+) cells and within the overlying epithelium (scale bar = 25 $\mu$ ). **D,E,F.** The staining of the tumor with Sox9 and K18 is also mutually exclusive and reveals a similar pattern to Sox9/Sox2 double staining (scale bar = 50 $\mu$ ). **G,H,I.** The Sox9 antibody labels Bowman's duct/gland cell nuclei of the OE, but within the tumor it co-labels with Tuj-1(+) cells. The arrow indicates a neuronal process. Scale bar = 25 $\mu$ .

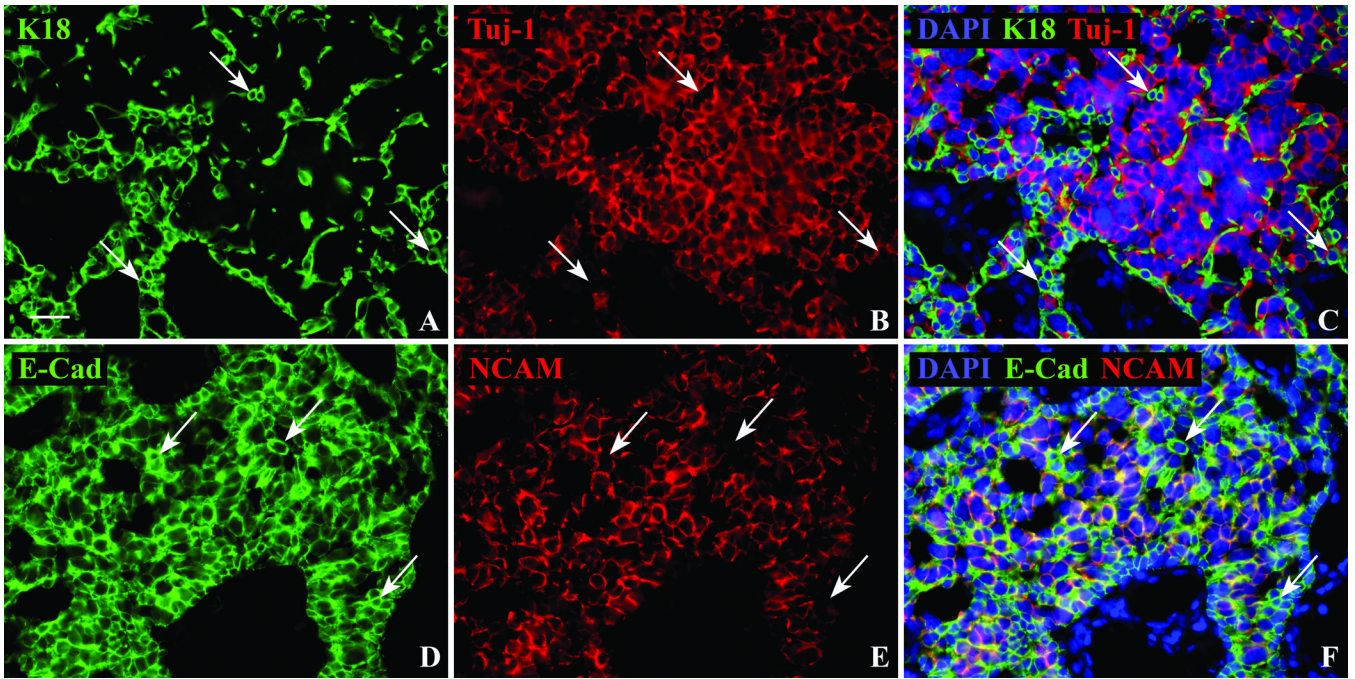


**Figure 8.**

Sox9(+)/Tuj-1(+) tumor cells do not follow the usual pattern of staining of olfactory epithelial gland cells. **A,B,C.** The separation of the tumor into two populations is confirmed using K18 and Tuj-1 antibodies. Similar to the two cell populations demonstrated with Sox2 and Sox9 antibodies, immunofluorescent labeling of cell cytoplasm and processes using K18 (**arrows**), does not co-label with the neuron-specific Tuj-1 antibody. **D,E,F.** E-Cad has a similar staining pattern as K18 in the epithelium labeling both gland and supporting cells, however within the tumor K18 is restricted to the Sox2(+)/Sox9(-)/Tuj-1(-) population while E-Cad labels the same NCAM(-) non-neuronal population (**arrows**) as well as the NCAM(+) neuronal population. **Scale bar** = 25 $\mu$ .

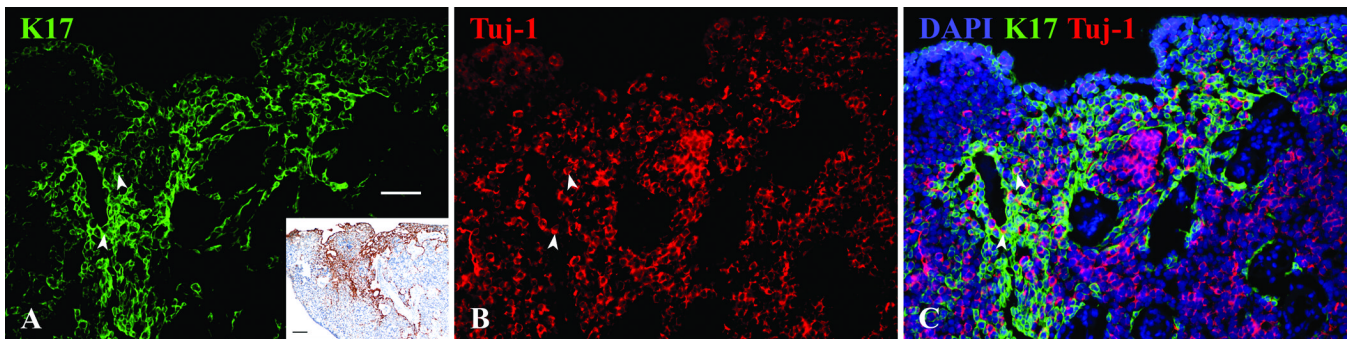


**Figure 9.**

**A.** The antibody to K17 labels only a portion of the tumor as shown with immunofluorescent staining and DAB at a lower magnification in the inset (inset **scale bar** = 100 $\mu$ ). **B,C.** Using double immunofluorescent staining with Tuj-1 a small number of cells are co-labeled with both antibodies (**arrowheads**), but most K17(+) cells seem to follow a pattern of staining similar to K18/Sox2 antibodies. **White scale bar** = 50 $\mu$ .

Table 1

## Antibody Details

Antibody	Species	Concentration	Company	Catalogue #	Antigen
Beta-Tubulin IV	Mouse	1:10000	Sigma	T7941	c-terminal synthetic peptide beta-tubulin IV
K17	Rabbit	1:1500	Abcam	ab53707	c-terminal synthetic peptide human keratin 17
K18	Mouse	1:3000	Invitrogen	18-0158z	human keratin 18 (45 kDa) polypeptide
K18	Rabbit	1:9000	Abcam	52948-100	c-terminal synthetic peptide human keratin 18
K5/6	Mouse	1:150	Chemicon	MAB1620	purified human keratin 5
E-Cad	Mouse	1:300	Invitrogen	13-1700	human E-Cadherin
EGFr	Sheep	1:200	UBI	06-129	recombinate human EGF receptor
G <sub>oif</sub>	Rabbit	1:500	Santa Cruz	sc-383	c-terminus of G <sub>o</sub> s/olf of rat origin
Hes1	Rabbit	1:2000	Generous gift from Dr. T. Sudo		hes-1 protein
Ki67	Rabbit	1:400	Epitomics	4203-1	c-terminal human Ki67
Mash1	Mouse	1:30	BD Biosciences	556604	recombinate full length rat Mash1
NCAM	Rabbit	1:2500	Generous gift from Dr. Covault		neural cell adhesion molecule
Notch1	Rabbit	1:250 – 1:50	Cell Signaling	D1E11	residues surrounding Pro2439 of a synthetic full-length peptide recognizing the transmembrane/intracellular region
OMP	Goat	1:12000	Wako	544-10001	rodent olfactory marker protein
p27	Mouse	1:5000	BD Biosciences	610241	aa 1-197 mouse Kip1
p63	Mouse	1:1000	Santa Cruz	sc-8431	aa 1-205 human p63
Pankeratin	Rabbit	1:2000	DAKO Cytomation	A0575	human keratins
Pax6	Rabbit	1:6000	Chemicon	AB5409	c-terminus synthetic human/mouse Pax6
PGP9.5	Rabbit	1:30000	Cedarlane	RA95101	human brain protein gene product 9.5
Sox2	Goat	1:100	Santa Cruz	sc-17320	c-terminus synthetic human Sox2
Sox9	Rabbit	1:2000	Millipore	AB5535	sequence CCTTGAG synthetic peptide from human Sox9
Tuj-1	Mouse	1:300	Covance	MMS-435P	rat brain beta-tubulin III

**Table II**

## Staining Characteristics by Cell Type

Cell Type	Structural Components	Transcription Factors	Signaling/Metabolic Activity/Adhesion
HBC	K5, K17, pankeratin	p63, Pax6, Sox2	EGFr
GBC		Mash1, Notch1, Sox2	
Immature OSN	Tuj-1		G <sub>olf</sub> , NCAM, PGP9.5
Mature OSN	Tuj-1		G <sub>olf</sub> , NCAM, PGP95, OMP
Sustentacular Cells	K18, pankeratin	Hes1, Pax6, Sox2	E-Cad, EGFr
Bowman's Duct/Glands	K18, pankeratin	Pax6, Sox9	E-Cad
Ciliated Respiratory	Beta-Tubulin IV		